NeuroImage 202 (2019) 116080

Contents lists available at ScienceDirect

NeuroImage

journal homepage: www.elsevier.com/locate/neuroimage

Prediction-based neural mechanisms for shielding the self from existential threat

Y. Dor-Ziderman [a,*,1], A. Lutz [b], A. Goldstein [a,c]

[a] Gonda Brain Research Center, Bar Ilan University, Ramat-Gan, Israel
[b] Lyon Neuroscience Research Center, INSERM, U1028, CNRS UMR5292, Lyon 1 University, Lyon, 69500, France
[c] Department of Psychology, Bar Ilan University, Ramat-Gan, Israel

A B S T R A C T

The human mind has an automatic tendency to avoid awareness of its mortality. How this protective mechanism is implemented at the neuronal level is unknown. Here we test the hypothesis that prediction-based mechanisms mediate death-denial by shielding the self from existential threat. We provide evidence that self-specific predictive processes are downregulated during the perception of death-related linguistic stimuli and that this mechanism can predict fear-of-death. Using a magnetoencephalography visual mismatch paradigm, we show that the brain's automatic prediction response to deviancy is eliminated when death words and self-face representations are coupled, but remains present when coupled to other-face or to negative words. We further demonstrate a functional link between how death impacts self-image vs. Other-image, and show that it predicts fear-of-death. Finally, we confirm this effect in a behavioral active inference experiment showing that death-related words bias perceptual judgment on facial self and other morphed video clips. Together these results lay out, for the first time, a plausible neural-based mechanism of death-denial.

1. Introduction

Everybody knows that they are going to die, right? The statistics regarding the likelihood of dying are undeniable. It is a 'fact of experience' (Heidegger, 1962). Yet, the human mind goes to great lengths to avoid awareness of its mortality. Death-denial has been empirically studied for more than thirty years and by hundreds of experiments, mainly under the Terror Management Theory (TMT, Greenberg et al., 1986) framework, using a wide array of behavioral manipulations (Burke et al., 2010; Pyszczynski et al., 2015). TMT has received much attention for revealing the dark side of death denial defenses, showing that they strip the human psyche of a degree of its freedom, where, unaware, it attempts to align itself with what it perceives as the salient cultural values (Pyszczynski et al., 2004) and adopts a prejudiced, intolerant and even aggressive attitude towards those falling outside its boundaries (Greenberg and Kosloff, 2008).

Neurocognitive investigation of how death reminders affect the brain has begun less than a decade ago (Henry et al., 2010). Some evidence has accumulated, associating decreased bilateral insula activity (fMRI studies: Han et al., 2010; Klackl et al., 2013; Shi and Han, 2013) to the processing of death-related (but not equally negative-valenced) linguistic stimuli. These authors have proposed this deactivation to reflect a decrease in the sense of one's self, based on a substantial body of work by Craig and colleagues (2009, 2010) who have related insula activity to 'self sentience', a global integrated representation of interoceptive signals in the body giving rise to subjective embodied self-awareness. While this interpretation is a promising way to look at how death concerns are managed by the brain, it should be treated with caution as it is based on a reverse-inference interpretation of brain activity to function (Poldrack, 2006), lacking the support of tasks or measures targeting specific neurocognitive mechanisms. In particular, the neurocognitive mechanism by which the brain 'denies' death is unknown. Specifically, we test the hypothesis that self-specific (Christoff et al., 2011) predictive processes are downregulated during the perception of death-related stimuli and that this mechanism can predict fear-of-death.

Predictive coding accounts view the brain as essentially a prediction machine which functions as a hierarchical generative model of the world following Bayesian probability principles (Barrett and Simmons, 2015; Clark, 2013). The brain is conceptualized to be a statistical organ, trying, to the best of its ability, to make sense of a world which is hidden from it by simulating (or statistically modeling) its inner (interoceptive) and outer (exteroceptive) workings in a manner which is open to correction by sensory feedback. Discrepancies between anticipated and actual sensory information, termed

* Corresponding author. Gonda Brain Research Center, Bar-Ilan University, Ramat-Gan, 52900, Israel.
E-mail address: yairem@gmail.com (Y. Dor-Ziderman).
[1] Current affiliation: Sagol Center for Brain and Mind, Interdisciplinary Center (IDC), Herzliya, Israel.

https://doi.org/10.1016/j.neuroimage.2019.116080
Received 17 February 2019; Received in revised form 25 July 2019; Accepted 6 August 2019
Available online 8 August 2019

'prediction errors', are reduced in one of two ways: either by updating the predictions so they better match the sensory evidence (perceptual inference), or by sampling the sensorium in a biased manner that fits the predictions (active inference). The process of updating top-down predictions (or prior beliefs) to accommodate bottom-up prediction errors has been shown to be functionally structured in the brain as descending and ascending neuronal signaling amid multiple levels of neural populations which encode statistical probabilities (Bayesian beliefs) representing world states (Bastos et al., 2012; Rao and Ballard, 1999).

Recent theoretical studies have suggested predictive coding accounts of embodied pre-reflective self experience (Limanowski and Blankenburg, 2013; Seth et al., 2011; Seth and Friston, 2016). Selfhood is argued to be formed by the integration of predictive interoceptive and exteroceptive signals, with low interoceptive sensitivity allowing modulation of self-other boundaries (Tajadura-Jiménez and Tsakiris, 2014; Tsakiris, 2017), possibly due to a lower precision-weighting (i.e., less reliability) of prediction error (Seth, 2013). A predictive coding account of self recognition has been suggested (Apps and Tsakiris, 2014) and recently validated (Sel et al., 2016) using a visual mismatch response (vMMR) paradigm. The MMR is an electrophysiological signal indexing the violation of a rule established by the repetition of sensory stimuli. It is widely considered as a perceptual prediction error signal interpreted within a predictive coding framework (Garrido et al., 2009; Lieder et al., 2013; Stefanics et al., 2014a; Winkler and Czigler, 2012). Sel et al. (2016) employed a vMMR paradigm that presented sequences of self or other (both familiar and unfamiliar) facial images disrupted by deviant images which were morphed to contain 33%, 66% or 100% of the unexpected face. vMMRs appeared at 170–300 ms post stimulus presentation for deviant self-images only and their amplitudes were proportional to the degree of prediction error (manipulated by morphing degree) and were unaffected by image familiarity, making a strong case for a self-specific automatic prediction response.

Building on this framework, we aim to demonstrate that this automatic prediction-based self-specific system fails when death is 'in the picture'. We hypothesize that this 'self bias reversal' is due to the encoding of a powerful prior associating the concept of death with the 'other' (non-self), rather than 'self'. This Bayesian 'belief', in turn, impacts the brain's self-specific system which is constantly and implicitly implementing a functional self/non-self (other) distinction in perception, action, cognition and emotion (Christoff et al., 2011). Thus incoming death cues tilt the self-other perceptual system towards the other, shielding the self from existential threat. We show that coupling death reminders (death-related words) and self-image in a vMMR paradigm diminishes the perceptual predictive capacity of the human brain and that this decrease is related to individual fear-of-death. This is corroborated by an additional behavioral experiment in which we used 'self' and 'other' face images and face-morphing techniques to outline an active inference mechanism which biases the self-specific system towards the 'other' when mortality is salient.

2. Experiment 1

To show that self-face prediction errors are not generated in the human brain under existential threat, we employed an adaptation of the study by Sel and colleagues (Sel et al., 2016), using magnetoencephalogram (MEG) recordings (n = 24) which have unique strengths in terms of millisecond source imaging (Baillet, 2017). We combined a vMMR face paradigm with linguistic priming of death-related or negative words as a control condition (matched for valence, arousal, concreteness, length and frequency with the death-related words, see Methods, Stimuli section and Table 1). Self and other face images served as standards (STD), and a 50% self-other morphed image served as a deviant (DEV) image for all conditions. We did not include a familiar condition, as Sel and colleagues (Sel et al., 2016), as well as others (Platek et al., 2006), have demonstrated that self-specific prediction errors cannot be attributed to the effects of familiarity. The paradigm used four conditions: death/self (DS), death/other (DO), negative/self (NS), and negative/other (NO). Our dependent measure was the vMMR, measured as the amplitude difference between event-related magnetic fields (ERF) elicited by deviant and by standard faces. The third image presentation in each sequence was used as standard in order to equalize the number of standards and deviants. At any time during the sequence, a target face (self, other or morphed) with sunglasses could appear matching the sequence type (SELF or OTHER) and location (STD or DEV). Subjects were instructed to press a button with their index finger as soon as a target image was detected (see Fig. 1). Hit rates as well as response latencies were collected. Beyond maintenance of participants' alertness and focus on the facial stimuli, these behavioral measures were included to rule out attention as a significant mediator.

The same deviant image, equally physically similar to both the 'self' and the 'other' image, was used in all conditions, assuring that any resulting vMMR differences between conditions would have to be *necessarily* attributed to the manipulated setting (or in other words, the experimentally-generated priors) onto which the deviant image was projected, rather than to properties relating to the deviant *per se*. We hypothesized that death salience would generate a context in which probabilistic representations of 'death is related to others (non-self)' would decrease the likelihood that incoming sensory stimuli (self-face) would be processed as self-related information. We expected the brain's predictive system to falter (a diminished vMMR effect) under existential threat when coupled with self-, but not with other-, perception, and that this self-other distinction would be unique to death-related (and not negative) stimuli.

2.1. Methods

2.1.1. Participants

Twenty four healthy participants (11 female, mean age 26.4 years, *SD* = 4.8) were recruited for experiment 1. Sample size was based on recent EEG (Kimura et al., 2012; Sel et al., 2016; Stefanics et al., 2012) and MEG studies (Xu et al., 2018) employing human faces as biologically-relevant stimuli in vMMN paradigms (Colonnello et al.,

Table 1
Word stimuli properties and ratings. Information provided for each word category (death, negative and neutral) include median and IQR values of Likert 1–7 scale ratings of valence, arousal, death-relatedness, and concreteness; as well as mean and *SD* of the words' frequency (in Hebrew) and length (number of letters).

(n = 36)	Valence	Arousal	Death-relatedness	Concreteness	Frequency	Length
Death	6.38 (.6) #	5.3 (.82) #	6.32 (.83) *	4.25 (1.45) #	632.27 (874.44) #	4.67 (1.33) #
Negative	6.24 (.56) #	5.2 (.58) #	1.9 (.52) *	4.25 (1.65) #	629.56 (1019.65) #	4.66 (1.55) #
Neutral	3.93 (.24)	3.39 (.55)	1.21 (.44) *	4.24 (1.95) #	630.44 (654.53) #	4.67 (1.11) #

Column cells sharing a # symbol are **not** significantly different ($p > .1$, BF = 0.243).
Column cells sharing a * symbol are significantly different ($p < .001$, BF > 1000).
Column cells **not** sharing a # or * symbol are significantly different ($p < .001$, BF > 1000).

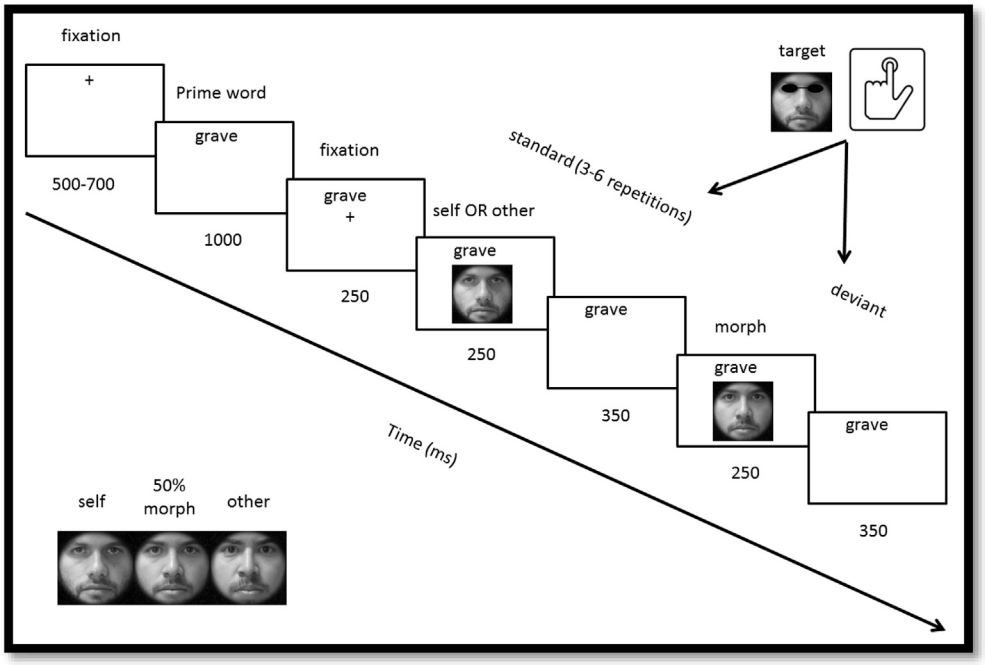

Fig. 1. Setup of Experiment 1. Time course and trial stimuli. Participants were shown a (death-related or negative) prime word for 1 s. After that, underneath the word, 3–6 repetitions of standard (either self or other faces) and then a deviant face (50% self-other morphs) were shown. Faces were shown for 250 ms followed by a blank image for 350 ms. Participants' task was to press a button when a target stimuli (face with sunglasses) was detected. There were 360 total trials delivered in 3 blocks. 90 target trials (randomly appearing), 4 conditions averaging of 67.5 trials per condition, 1:4.5 standard to deviant ratio.

2013; Heinisch et al., 2013; Keenan et al., 2000; Kita et al., 2010), and in addition, on the sample sizes in neurocogntive mortality salience studies (a review yielded a mean subject number of 21.2). Participants were recruited by flyers posted online and throughout campus, to participate in a "face recognition under emotional load" experiment. All participants were right-handed, fluent Hebrew speakers, with normal or corrected vision and with no self-reported history of neurological or psychiatric disorders. All the performed procedures are in compliance with the Code of Ethics of the World Medical Association (Declaration of Helsinki) and were approved by the Research Ethics Board of Bar-Ilan University. The participants gave their written consent, and were financially compensated for their time.

2.1.2. Face Stimuli

Consisted of Six grey-scaled pictures of faces (425 × 405 pixels) with neutral expressions were presented centrally on a black foreground, using E-prime2 software (Psychology Software Tools). Face images included the participant's face (SELF), a gender-matched individual (OTHER) and a morphed face that contained 50% of the participant's face and 50% of the gender-matched individual (MORPH). The morph images were created using FantaMorph4 (Abrosoft FanatMorph Software). In addition, target images were created by adding black sunglasses to the three images described above, yielding a total of six images per subject. All photographs were taken in a designated location against a white wall under similar lighting conditions. Non-facial features were masked out using a round black outline and the images were equalized for low level image properties (luminance, contrast, intensity and spatial frequency) using the SHINE toolbox (Willenbockel et al., 2010).

2.1.3. Word stimuli

Consisted of 108 words of three categories (36 words in each): death-related (DEATH), negative (NEG) and neutral (NEUT). The words were selected from an existing database (Shay, 2016) using an in-house evolutionary algorithm designed to optimize word-selection so that the word categories would be (1) equivalent in terms of word frequency (in Hebrew, based on Google search), length (number of letters), and concreteness (subjective ratings), and that (2) the DEATH and NEG stimuli would also be equal in terms of valence and arousal ratings, but different in their degree of relation to death (on Likert 1–7 scales, ratings obtained from an independent population). Stimuli median, interquartile range (IQR) and significance, using the Mann-Whitney *U test*, as well Bayes Factors (BF), are summarized in Table 1 for Likert-type scales variables (valence, arousal, death-relatedness, concreteness). For the frequency and length variables, stimuli means, standard deviations, and significance using independent-samples *t-test*, as well BF, is supplied. In Experiment 1 only the DEATH and NEG categories were used.

2.1.4. Procedures

We implemented a fully-randomized 2 × 2 design with PRIME (DEATH or NEGATIVE) and IDENTITY (SELF or OTHER) as within-subject factors. Each trial started with the presentation of a small fixation cross on the screen for 500–700 ms and then a prime word (DEATH or NEG) for 600 ms. After that, directly underneath the prime word, a central cross appeared for 250 ms and then a sequence of face images. Each sequence consisted of identical 3–6 standard (SELF or OTHER) face images and then a deviant face (MORPH). Each face was presented for 250 ms with a stimulus onset asynchrony of 600 ms. At any point during the sequence, a target face could appear matching the sequence type (SELF or OTHER) and sequence location (standard or deviant). Subjects were instructed to press a button with their index finger as soon as a target image was detected. The experiment was divided into three blocks, and preceded by a practice block. Between each block participants were requested to close their eyes and rest. Each block consisted of 120 trials (prime word plus the faces sequence), 30 of which included targets and were not included in the ERF analysis. Regarding the non-target sequences, there was an average of 67.5 trials per condition, 82% of images were standard and 18% were deviant. The task took around 40 min to complete (including the practice and rest periods). See Fig. 1 for a visual depiction of the study setup.

2.1.5. Self-report questionnaires

Twenty minutes prior to entering the MEG room and commencing the vMMR study (experiment 1), participants completed a self-report measure of fear of death and a control fear of dental pain measure. We used the Fear of Personal Death Survey (FPDS, Florian and Kravetz, 1983), which is the survey most commonly used to manipulate mortality salience (Burke et al., 2010). The FPDS consists of 31 questions which are normally answered on a 7-point Likert-type scale ranging from 1 (totally

incorrect for me) to 7 (totally correct for me). As we were interested in measuring response latencies (RT), we modified the FPDS so that it was administered as a forced-choice 2-point yes-no computerized questionnaire, answered using the index and middle fingers, respectively. The questions were presented randomly. After answering each question, a cross appeared for 2 s, and then the next question appeared. Our dependent measures were the RTs. The RT for the first question was not considered. In order to confirm that slower response latencies indicated an increase in mortality salience –related affective load, we constructed a fear-of-dental-pain questionnaire based on previously gathered first person reports. Dental pain salience is the most widely used control for mortality salience (Burke et al., 2010). The questionnaire was equal in length to the FPDS (same number of questions and words), and was administered in a similar manner to the FPDS with order counter balanced. As expected, the FPDS RT's were significantly longer than those of the fear-of-dental-pain questionnaire (Mdiff = 485 s, SEMdiff = 210; $t(23) = 2.31$, $p = .03$). We were not concerned that completing the fear of death/dental-pain questionnaires would induce psychological demand characteristics which would bias the MEG experiment's results because (1) the MEG's overt task (identifying faces with sunglasses), which could plausibly be suspect of bias, showed no differences between death and negative stimuli, while (2) the dependent variable of interest (the vMMR), is a fast, automatic implicit measure working at the level of perception which is not likely to be influenced by demand characteristics, and in any case, (3) the questionnaires probed both death-related and negative fears in counterbalanced order, with similar instructions and suggested import assigned to both.

2.1.6. MEG Data Collection

Ongoing brain magnetic activity was recorded (sampling rate, 1017.23 Hz, online 0.1–400 Hz band-pass filter) using a whole-head 248-channel magnetometer array (4-D Neuroimaging, Magnes 3600 WH) in supine position inside a magnetically shielded room. Reference coils located above the head oriented by the x, y, and z axes were used to remove environmental noise. Five coils were attached to the participant's scalp for recording the head position relative to the 248 sensor-array. The head shape was manually digitized using a Polhemus Fastrak digitizer. A photosensitive diode on the screen recorded the onset time of visual stimuli. A response box was used for collecting manual responses.

2.1.7. MEG Data Cleaning

The data were analyzed using the FieldTrip toolbox (Oostenveld et al., 2011) as well as MATLAB R2013b (MathWorks, Natick, MA, USA) custom-made analysis scripts. External noise (e.g., power-line, mechanical vibrations), jumps in the MEG signal (caused by the SQUID electronics), and heartbeat artifacts were removed from the data using a predesigned algorithm (Tal and Abeles, 2013). Two bad channels were detected and excluded from further analysis. Data were segmented into 600 ms epochs (100 ms before face presentation to 500 ms after), the maximal length possible without inter-trial overlap. Data epochs of interest were checked for artifacts using a that involved (1) Using a semi-automatic routine in which the data were 60 Hz high-pass-filtered for detecting and rejecting trials containing muscle artifacts. (2) Running an independent component analysis (Bell and Sejnowski, 1995) to remove from the data any remaining variance related to eye blinks, eye movements and heartbeat artifacts (Jung et al., 2000). (3) Finally, the data were visually inspected and any remaining trials with artifacts were removed manually.

2.1.8. Event related fields analysis and statistics

Data were analyzed using FieldTrip (Oostenveld et al., 2011) as well as MATLAB R2013b (MathWorks, Natick, MA, USA) custom-made scripts. Event-related fields (ERFs) were calculated by first low-pass filtering the data using a two-pass Butterworth filter with a filter order of 4 and a frequency cutoff of 40 Hz. ERFs were baseline corrected using an interval of 100 ms before faces presentation. A planar gradient transform was then calculated (Bastiaansen and Knösche, 2000) prior to averaging. Using planar gradients simplifies the interpretation of the sensor-level data as it typically places the maximal signal above the source (Hämäläinen et al., 1993). We avoided using the grand average data to manually select components' time windows and electrode sites, as this has been shown to often yield significant but bogus results (Luck and Gaspelin, 2017). Instead, we analyzed the data in an unbiased, data driven manner, consisting of three stages of finding the time points of interest (TOI), then the sensors of interest exhibiting the effect (SOI), and finally calculating between condition statistics on the time- and space-resolved data. To avoid circular analysis (Kriegeskorte et al., 2009), orthogonal contrasts were used (Kilner, 2013; Litvak et al., 2011; Luck and Gaspelin, 2017) for data selection (Finding TOI/SOI stages) and inference (Comparing the different conditions stage). As orthogonal contrasts may still be biased when using unbalanced samples (Kriegeskorte et al., 2009), we equalized the number of trials for each condition per subject before averaging over them. This method keeps the selection stage completely uninformed about what the conditions are and does not to inflate type I errors (as shown in Brooks et al., 2017, simulation 1).

2.1.8.1. Finding the TOI. For each participant, the standard and deviant trials were averaged over all conditions, sensors and trials, and the time points in which standard trials were statistically different (two-sample *t-tests*, $p < .05$ threshold) from deviant trials were calculated. To control for spurious results, only significant sequences of more than twenty consecutive time-points were considered.

2.1.8.2. Finding SOI. For each participant, standard and deviant trials were averaged over the time dimension in accordance with the TOI determined in step 1 and over all conditions, but not over the trials and sensors (spatial dimension). These were statistically compared (using independent samples *t-tests*), what resulted in a 2D 248-sensor *t-value* distribution for each participant. These were pooled over all participants and statistically compared between subjects using second-level nonparametric cluster-based permutation *t-tests* on pooled *t-values* (Maris and Oostenveld, 2007a). The resulting significant sensor clusters were defined as the sensors of interest (SOI).

2.1.8.3. Comparing the different conditions. Finally, for each subject we collapsed ERF power values over the SOI (step 2) and within the TOI (step 1), and computed difference waveforms (deviant – standard trials). This yielded a total of four values for each subject corresponding to a 2×2 design (PRIME x IDENTITY). These were subjected to a 2×2 repeated-measures ANOVA. Post-hoc one-sampled and paired-sample *t-tests*, pearson correlations and Bayes Factors (BF, Dienes, 2014) using a Cauchy distribution with scale $= 1/\sqrt{2}$. Bayes Factor is an indicator of the relative evidence for one theory over another. Importantly, it provides a coherent approach to determining whether non-significant results support a null hypothesis over a theory, or whether the data are just insensitive. Bayes Factor between 3 and 10 (1/3–1/10) are said to provide moderate evidence for a theory (null hypothesis). Frequentist statistics were computed using SPSS (IBM statistics version 21), and Bayes Factors were computed using R (jamovi project version 0.9, https://www.jamovi.org).

2.1.9. Nonparametric cluster-based permutation statistics

(Maris and Oostenveld, 2007b) were used to assess whether there were significant spatial clusters of differential ERF activity. This type of test controls the type I error rate in the context of multiple comparisons by identifying clusters of significant differences over space. This approach, which was implemented both at the sensor and source levels, was chosen as it makes no assumptions on the underlying distribution, and is unaffected by partial dependence between neighboring sensors/-voxels. In addition, this approach has been shown to yield nominal

(non-inflated) false-positive rates for spatial extent (Eklund et al., 2016). The cluster-level statistics, defined as the sum of *t-values* within each cluster, were evaluated under the permutation distribution of the maximum (minimum) cluster-level statistic. This permutation distribution was approximated by drawing 1000 random permutations of the observed data. The obtained *p-values* represent the probability under the null hypothesis (no difference between the conditions) of observing a maximum (minimum) cluster-level statistic that is larger (smaller) than the observed cluster-level statistics.

2.1.10. Source localization

Sources of evoked activity were identified using a time-domain beamforming approach on the magnetometers sensor data (linearly constrained minimum variance (Van Veen et al., 1997). We looked at the difference in average activity over the TOI elicited by the standard versus deviant facial images. For each participant, a single shell brain model was built based on a template brain (Montreal Neurological Institute), which was modified to fit each participant's digitized head shape using SPM8 (Welcome Department of Imaging Neuroscience University College London,www.fil.ion.ucl.ac.uk). The participant's brain volume was then divided into a regular grid. The grid positions were obtained by a linear transformation of the grid positions in a canonical 1 cm grid. This procedure facilitates the group analysis because no spatial interpolation of the volumes of reconstructed activity is required. For each grid position, the lead field matrix was calculated according to the head position in the system and the forward model. A common spatial filter was then constructed for each grid point using the covariance (calculated over the whole trial and including all trials of all conditions) and the lead field matrices. Single trial source power estimates were calculated based on single-trial covariance matrices and the common spatial filter. For each subject, we statistically compared the difference between the standard and deviant faces for each condition separately, what resulted in a 3D *t-value* distribution of the vMMR effect for each condition. These distributions were then pooled over all participants and subjected to second-level nonparametric cluster-based permutation statistics on pooled *t-values* as described earlier.

2.2. Results

Comparing standard and deviant trials over all conditions, sensors

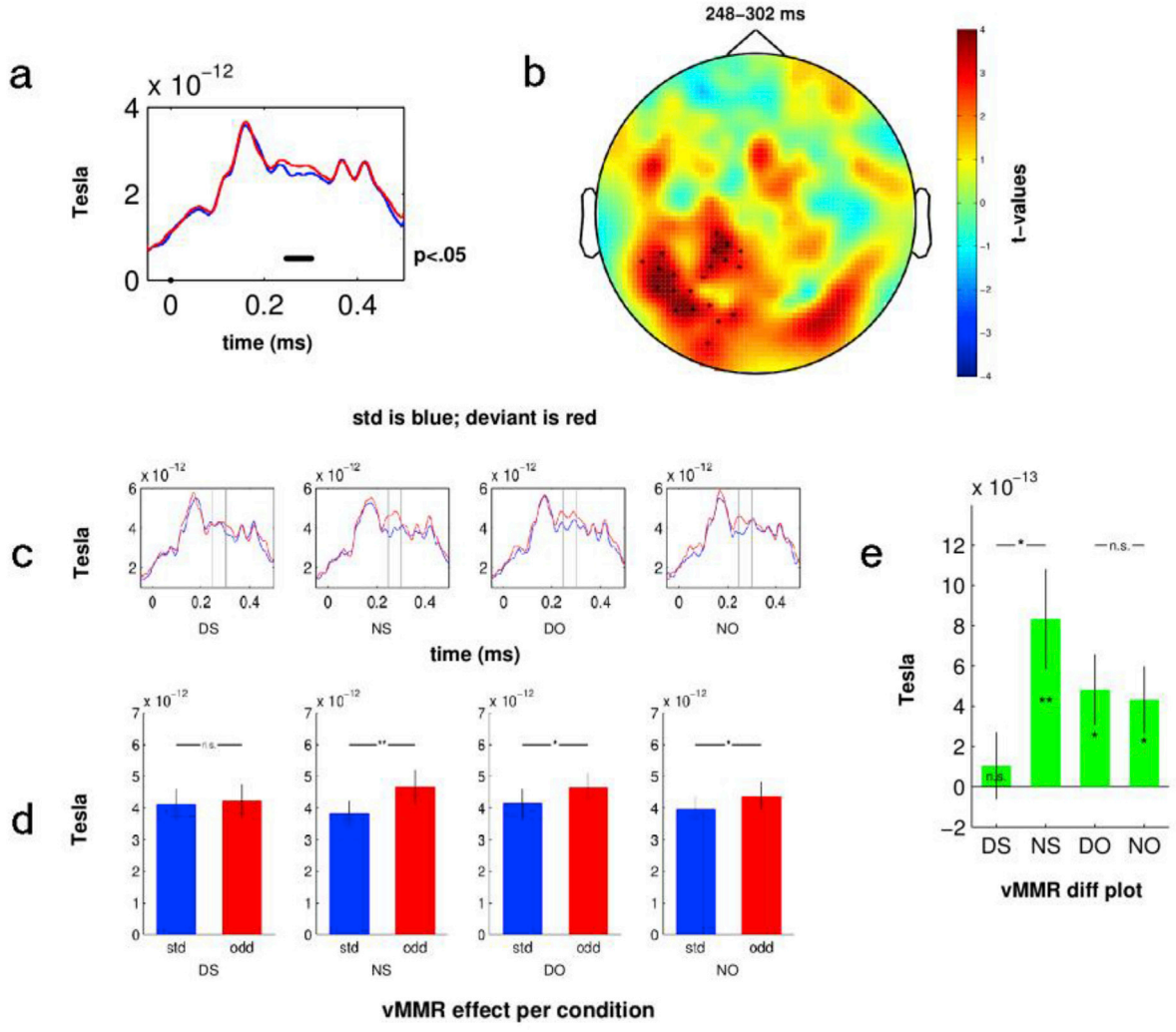

Fig. 2. ERF vMMR sensor-level results. (a) Event-related fields elicited by standards (blue) and deviants (red) averaged over all sensors. Significant time points ($p < .05$) are marked by black dots (248–302 ms post stimulus). (b) Topographical map of the deviants – standards (*t-values)* averaged over the time window of significance. Sensors in the significant cluster are marked by bold stars. (c) Event-related fields elicited by standards (blue) and deviants (red) in the significant cluster per condition. Time points of interest are between the 2 grey lines. (d) Mean cluster ERF amplitude over the vMMR time window in each condition. (e) vMMR difference plots (deviant minus standard) per condition. * = $p < .05$; **$p < .01$, *n. s.* = not significant.
AbbreviationsERF = event related fields; vMMR = visual mismatch response; DS = death_self; NS = negative_self; DO = death_other; NO = negative_other; std = standard trials (in blue); dev = deviant trials (in red).

and trials indicated a significant time-window of interest between 248 and 302 ms after stimulus presentation (see Fig. 2a), in line with other MEG/EEG face vMMR studies (Kimura et al., 2012; Sel et al., 2016; Vogel et al., 2015; Xu et al., 2018). A nonparametric cluster-based permutation test revealed a significant left posterior-temporal cluster (consisting of 21 sensors, $p = .002$. See Fig. 2b). Fig. 2c shows the standard and deviant time-courses, averaged over the significant sensors, for each condition separately. A repeated-measures 2×2 (PRIME x IDENTITY) ANOVA for the time- and sensor-resolved ERFs revealed no significant effects for IDENTITY ($p = .955$) and a marginally significant result for PRIME ($p = .071$). Consistent with our hypothesis, PRIME x IDENTITY yielded a significant interaction ($F(1,23) = 5.46$, $p = .028$, $\eta_p^2 = 0.19$).

As seen in Fig. 2d and e, post-hoc analyses of this interaction indicated a significant vMMR effect for the NS ($t(23) = 3.39$, $p = .003$, $d = 0.69$, $BF = 15.6$), NO ($t(23) = 2.64$, $p = .015$, $d = 0.54$, $BF = 3.52$), and DO ($t(23) = 2.78$, $p = .011$, $d = 0.57$, $BF = 4.61$) conditions, but not for the DS condition ($t(23) = 0.63$, $p = .53$, *n. s.*, $BF = 0.26$). Importantly, the DS condition evidenced a Bayes Factor of 0.26, indicating substantial evidence in favor of a true non-effect. Fig. 2e shows the vMMR difference scores (measured as DEV minus STD) for each condition. As can be seen, the vMMR measures for SELF differ as a function of the PRIME, while vMMRs for OTHER do not. The vMMR of the NS condition was significantly higher than the DS one ($t(23) = 2.47$, $p = .021$, $d = 0.5$, $BF = 2.59$). In contrast, there was no statistical difference between the NO and DO ($t(23) = -0.28$, $p = .78$, *n. s.*, $BF = 0.22$). Altogether, the vMMR reflected a reduced perceptual predictive process only when presentation of death-words coupled to self-image.

In order to show a functional relation between how death impacted self-image vs. Other image, we ran a correlation analysis between the death vMMRs (DS and DO). As can be seen in Fig. 3, the results indicated a negative correlation between the DS and DO conditions ($r = -0.41$, $p = .047$). This means that smaller the DS vMMR tended to be, the larger the DO vMMR tended to be, implying a functional inverse relationship between how death impacts self-image vs. Other-image. As a control, we also ran a correlation analysis between the negative vMMRs (NS and NO), which yielded non-significant results ($r = .25$, $p = .23$). The two correlation coefficients were significantly different (delta $r = -0.66$, $p = .012$).

To further investigate the functional meaning of how death impacts perception of self vs. Other stimuli, we constructed a death-denial index (DDI), computed by subtracting the DS from DO vMMRs. We examined its relationship with a self-report measure of fear-of-death, as well as the response latencies (RT) for completing it. As a control analysis, we computed a comparable "negativity" index (NI) by subtracting the NS from the NO vMMRs. For this analysis, we used the score to a yes/no version of the fear of personal death survey (FPDS, a validated questionnaire consisting of 31 items (Florian and Kravetz, 1983)). Based on pilot analyses (see Methods, Self-report Questionnaires section), we attributed longer RTs to an increased affective load. As shown in Fig. 4, we found a correlation between the DDI and the RT measure ($r = 0.62$, $p = .001$). The NI, by comparison, showed no significant correlation ($r = -0.08$, $p = .71$, *n. s.*). The DDI was a significantly better predictor of the FPDS RT measure than the NI (Steiger test, delta $r = 0.7$, $p = .001$). These findings strongly link our neurophysiological marker of death-denial to fear-of-death.

Next, to refine the functional interpretation of these findings, we analyzed the source-localized vMMR effect. Comparing NS to DS yielded significant clusters of higher activity in the NS condition (see Fig. 5) replicating the results by Sel et al. (2016) indicating temporal and limbic areas, including occipito-temporal (including the ventral fusiform gyrus), anterior temporal, right medial temporal, and anterior cingulate cortex (ACC) regions. In addition, the results indicated right inferior frontal and prefrontal activations including the ventromedial prefrontal cortex (PFC) and medial orbitofrontal cortex (OFC), in line with the vMMR literature in general (Hedge et al., 2015), vMMR of biologically relevant stimuli (Kimura et al., 2012), and self face recognition studies (Miyakoshi et al., 2010; Platek et al., 2008). See Table 2, for more information on the regions involved. In contrast, no significant differences in activation appeared in the NO to DO comparison.

3. Experiment 2

In experiment 1, we suggested a death-denial mechanism implemented as a reduction in the brain's capacity to cast self-perception predictions (Garrido et al., 2009; Stefanics et al., 2014b) when coupled with death linguistic representations. In a second experiment, we hypothesized that biased sampling of the sensorium, an active inference mechanism attributing death to the other (non-self), served as a defense against existential threat. To test this hypothesis, we designed a fully-randomized 2×3 behavioral experiment ($n = 32$) based on an identity-change task on self and other morphed video clips under death-related, negative and neutral priming (see Fig. 6 for the study setup, and Methods Stimuli section, for more information on stimuli). Each morphed video clip displayed a face (either the subject's own or a gender-matched other's) gradually changing to the point where it no longer represented its original identity. Subjects were instructed to press a button at the precise point when they felt the identity of the face changed: when it was no longer them (in SELF clips), or when it was no longer the other (in OTHER clips). We hypothesized longer response latencies for detecting identity change in OTHER clips under death, but not negative, priming, as a means for actively biasing death representations to be associated with the other.

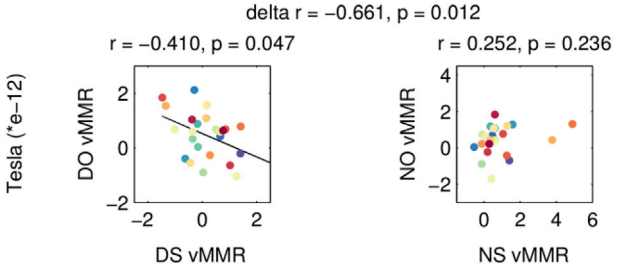

Fig. 3. Death and negative vMMR correlations. Correlation plots of DS vMMR and DO vMMR (left), and the NS vMMR and NO vMMR (right). y and x -axes values are in Tesla (10^{-12}). Pearson coefficients and p values indicating significance are provided. Linear lines are fitted to significant correlations only. Steiger test values for significant differences between the correlations appear on top.

Abbreviations: vMMR = visual mismatch response; DS = death_self; NS = negative_self; DO = death_other; NO = negative_other.

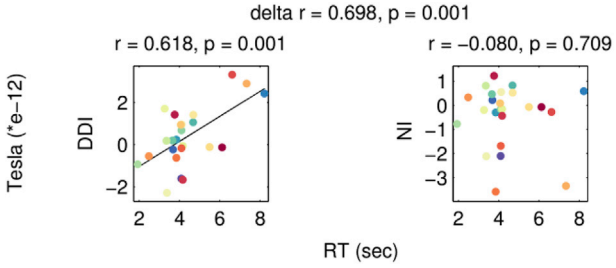

Fig. 4. MEG and fear-of-death correlates. Correlation plots of response latencies to FPDS items for DDI (left) and NI (right). y-axis values are in Tesla (10^{-12}), x-axis values are in seconds. Pearson coefficients and p values indicating significance are provided. Linear lines are fitted to significant correlations. Steiger test values for significant differences between correlations appear on top.

Abbreviations: FPDS=Fear of Personal Death Survey; RT = response time; vMMR = visual mismatch response; DS = death_self; NS = negative_self; DO = death_other; NO = negative_other.

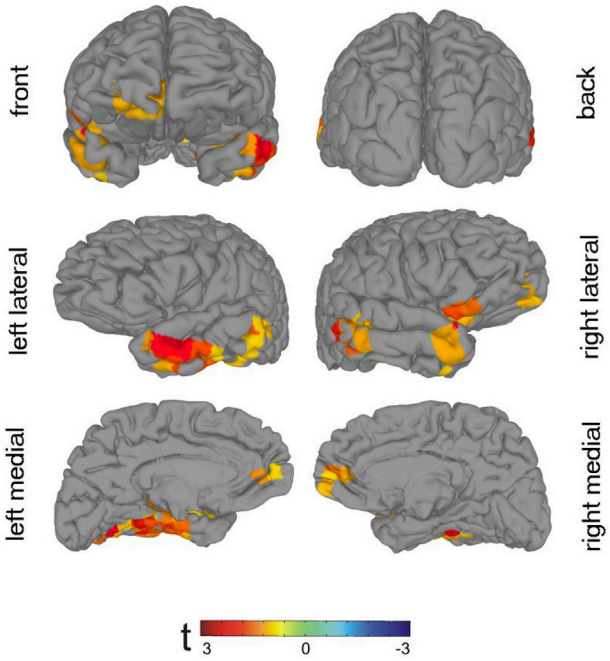

Fig. 5. Source estimates of NS vs. DS vMMR. Front (top left), back (top right), lateral (middle row), and medial (bottom row) views of the significant NS > DS vMMR clusters. Warm colors indicate positive *t-values*; cold colors indicate negative *t-values*.

Table 2
Source estimates of NS vs. DS vMMR. Information supplied includes total number of voxels, hemispheric overlap, peak voxel coordinates and brain regions involved. TT Daemon atlas was used. Due to poor resolution and signal leakage to non-brain regions, overlap percentages do not add up to 100%.

	Brain regions Talairach-Tournoux Atlas	% of cluster
Cluster 1 (78 voxels) Peak voxel (LPI) x(50) y(35) z(0)	L. Parahippocampal Gyrus	14.2%
	L. Middle Temporal Gyrus	12.0%
	L. Culmen	8.2%
	L. Fusiform Gyrus	8.0%
	L. Superior Temporal Gyrus	6.1%
	L. Inferior Temporal Gyrus	4.0%
Cluster 2 (17 voxels) Peak voxel (LPI) x(-30) y(45) z(-30)	R. Middle Temporal Gyrus	41.5%
	R. Culmen	10.0%
	R. Superior Temporal Gyrus	8.4%
	R. Fusiform Gyrus	5.4%
	R. Parahippocampal Gyrus	5.3%
Cluster 3 (14 voxels) Peak voxel (LPI) x(-50) y(-25) z(-20)	R. Superior Temporal Gyrus	25.8%
	R. Inferior Frontal Gyrus	18.7%
	R. Middle Temporal Gyrus	2.3%
Cluster 4 (7 voxels) Peak voxel (LPI) x(-10) y(-55) z(0)	R. Medial Frontal Gyrus	42.1%
	R. Superior Frontal Gyrus	25.5%
	R. Anterior Cingulate	16.3%

3.1. Methods

3.1.1. Participants

Thirty two healthy participants (22 females, mean age 23.32 years, *SD* = 2.45) were recruited for experiment 2. Sample size was based on previous studies employing video-morphing on self-other facial stimuli, allowing for the added present-study complexity of introducing linguistic primes. Participants were recruited by flyers posted online and throughout campus, to participate in a "face recognition under emotional load" experiment. All participants were right-handed, fluent Hebrew speakers, with normal or corrected vision and with no self-reported history of neurological or psychiatric disorders. All the performed procedures are in compliance with the Code of Ethics of the World Medical Association (Declaration of Helsinki) and were approved by the Research Ethics Board of Bar-Ilan University. The participants gave their written consent and were financially compensated for their time.

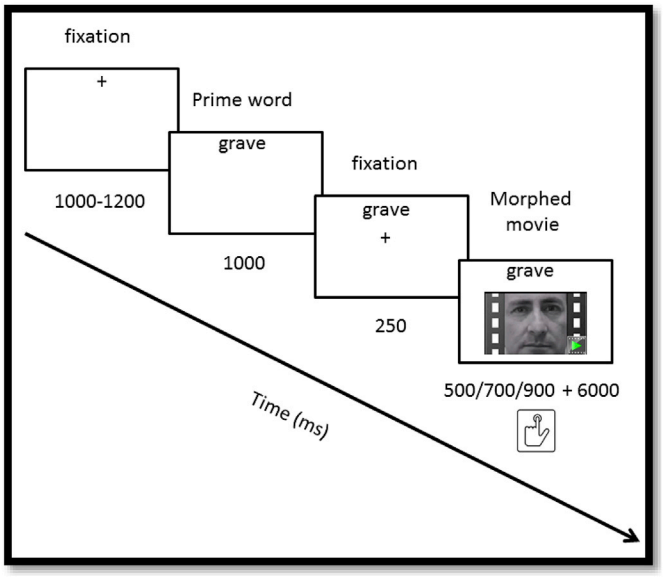

Fig. 6. Setup of Experiment 2. Time course and trial stimuli. Morphed video clips showed the participant's or a gender-matched other's face gradually morphed into one of three possible gender-matched strangers. Clips were 6 s long and were preceded by a 500/700/900 ms static phase (for a total of 18 morph clips per subject). Participants were instructed to press a button during the video clips to indicate when the identity of the face in the morphed clips changed (when one's own/other's face no longer reflected him/her). In the upper part of the screen a prime word (death, negative or neutral) appeared before each clip and stayed visible throughout the trial. There were 324 total trials, randomly delivered in 3 blocks, equally divided between death, negative and neutral primes for self and other morphed clips (6 conditions, 54 trials each).

3.1.2. Stimuli

Included the three word lists detailed above: DEATH, NEG and NEUT. The visual stimuli consisted of grey-scale, 1280 × 720 pixels, 23 frames-per-second, 6-s morphed video clips presented centrally on a black foreground in which one's own facial image (SELF) or that of a gender-matched other (OTHER) changed its identity to one of three gender-matched faces. In order to further vary the stimuli and counter automaticity in responses, we also used three different video-clip lengths implemented by a 500, 700 or 900 ms period in which the face remained static before morphing begun. This yielded a total of nine morphed SELF clips, and nine morphed OTHER clips, for a total of eighteen clips per subject. The morphed video clips were created using FantaMorph4 software. All the photographs used for creating the morphed clips were taken in a designated location against a white wall under similar lighting conditions with subjects exhibiting a neutral expression. Faces were cropped so that hair, ears and neck were not included in the image. Stimuli were presented using E-prime2 software (Psychology Software Tools).

3.1.3. Procedure

We implemented a fully-randomized 2 × 3 design with IDENTITY (SELF or OTHER morph video clips) and PRIME (DEATH, NEG, or NEUT prime words) as within-subject factors. Each trial started with a cross appearing for 1–1.2 s, after which it was replaced by a prime word (DEATH, NEG or NEUT) for 1 s. Then, underneath the prime word (which stayed on the screen) one of the morphed clips (randomly chosen) begun to play preceded by a 250 ms cross located at the picture's center. Each morphed video clip displayed a face (either one's own or a gender-matched other's) gradually changing to the point where it no longer represented its original identity. Subjects were instructed to press the SPACEBAR button at the precise point when they felt the identity of the face changed: when it was no longer them (in SELF clips), or when it was longer the other (in OTHER clips). Pressing the button cleared the screen and a new trial begun. The experiment was divided into three blocks, and was preceded by a practice block. Between each block participants were requested to rest for a few minutes. Each block consisted of 108 trials, equally divided between the prime conditions, for a total of 54 trials per condition and an overall total of 324 trials. The whole task including the practice and rest periods took about 40 min to complete. Study setup is illustrated in Fig. 6.

3.1.4. Data analysis

Data were analyzed using MATLAB R2013b (MathWorks, Natick, MA, USA), frequentist statistics were computed using SPSS (IBM statistics version 21), and Bayes Factors were computed using R (jamovi project version 0.9, https://www.jamovi.org). First we subtracted from each clip the initial duration in which it remained static (500, 700, or 900 ms). We then examined the data for outlier errors using scatter and Q-Q plots (Aguinis et al., 2013). Outlier response latencies were removed following Ratcliff (1993) who showed that for ANOVA analyses, greatest power is obtained by a eliminating a small percentage of response times longer than some specific cutoff value. Furthermore, the author further suggested using standard deviations as cutoff values for studies with small sample sizes and large variability between subjects (as in the present study). Accordingly, for each subject we excluded outlier latencies using a pre-determined (prior to analyzing the data) cutoff value of +/− 3 *SD*s. Finally, we checked the robustness of the outlier removal procedure by trying outlier removal using a range of other non-extreme cutoff values (+/− *SD*s of 2, 2.5, 3.5, 4) to ensure that the effect (*F* values) remained significant (Ratcliff, 1993). This procedure was done for SELF and OTHER trials separately, as the average differences between SELF and OTHER clips were an order of magnitude larger (~500 ms) than the differences between SELF by PRIME conditions and OTHER by PRIME conditions (~50 ms). Overall, 1.15% of the trials were thus excluded, with the 2 × 3 (IDENTITY x PRIME) number of trials distributions not significantly different from each other ($F(2,30) = 0.75$, *n. s.*). Statistics were computed using repeated–measures ANOVAs. Post hoc analyses were conducted using paired-samples *t*-tests, and Bayes Factors using the default prior distribution (Cauchy distribution with scale $= 1/\sqrt{2}$).

3.2. Results

A repeated–measures 2 × 3 (IDENTITY x PRIME) ANOVA on response latencies indicated a large significant main effect for IDENTITY ($F(1,31) = 42.1$, $p < .000$, $\eta_p^2 = 0.58$), but not for PRIME ($F(2,30) = 0.8$, $p = .44$, *n. s.*). SELF morph clips (M = 3120 ms SEM = 104 ms) were much shorter ($t(31) = -6.49$, $p < .000$) than OTHER clips (M = 3582 ms, SEM = 133 ms), consistent with the well-documented self-advantage effect (Apps and Tsakiris, 2014; Brédart et al., 2006; Keenan et al., 2000; Pannese and Hirsch, 2010). Most importantly, there was a significant IDENTITY × PRIME interaction ($F(2,30) = 4.4$, $p = .017$, $\eta_p^2 = 0.12$). As seen in Fig. 7a, and in line with our hypothesis, responses in OTHER morph clips after a DEATH prime word were significantly longer than after a NEG prime word (Mdiff = 54 ms, SEMdiff = 20 ms; $t(31) = 2.7$, $p = .011$, $d = 0.47$, BF = 3.93), and longer at a trend level than after a NEUT prime word (Mdiff = 42 ms, SEMdiff = 23 ms; $t(31) = 1.8$, $p = .07$, BF = 0.86). For SELF morph clips, comparisons of DEATH to NEG were not significant (Mdiff = −23 ms, SEMdiff = 15 ms, $t(31) = -1.54$, $p = .13$, *n. s.,* BF = 0.55), and neither were comparisons of DEATH to NEUT (Mdiff = −15 ms, SEMdiff = 18 ms; $t(31) = -0.87$, p = .39, *n. s.,* BF = 0.27). As in experiment 1, we constructed a death-denial index (DDI, OTHER minus SELF RTs), as well as negativity (NegI) and neutral (NeutI) indices. As shown in Fig. 7b, both the DDI and NegI yielded significant effects (1 sample *t*-test) but in opposite directions ($t(31) = 2.5$, $p = .017$, $d = 0.45$, BF = 2.83 and $t(31) = -2.6$, $p = .015$, $d = -0.45$, BF = 3.1, respectively), while NeutI did not ($t(31) = -0.76$, $p = .45$, *n. s,* BF = 0.24). The DDI behaved similarly to the one shown in experiment 1, strengthening the novelty and specificity of the finding. We did not predict the significant opposite NegI direction (shorter RT during OTHER than SELF), which could reflect the well-known positive bias for self (Sedikides and Gregg, 2008): negative information might be used to a lesser degree to update the self, but more rapidly to update the other. In any case, the opposite directions of negative and death-related DDI effects are a clear indicator that the death-related findings cannot be explained by valence and arousal features alone.

4. Discussion

The objective of the study was to establish that prediction-based neurocognitive mechanisms were actively involved in the denial of death, shielding the self from existential threat by attributing death to the 'other' (or non-self). We first addressed this goal by showing that the brain's automatic prediction system, measured using a biologically-relevant visual mismatch response paradigm (vMMR), failed at predicting self-related information, but not other-related information, when under existential threat (Experiment 1). We interpret this result as indicating a low-level perceptual incompatibility between bottom-up visual information (self-face image) indicating self, and top-down predictions (death priming) indicating the other. This incompatibility may have resulted in a reduced encoding of precision or expected uncertainty to the prior (i.e., a less reliable signal), which then lowered the weight of the error prediction (Seth, 2013; Seth and Friston, 2016). Thus the brain did not form a sensory prediction regarding the ensuing visual stimuli, leading to a null vMMR effect. This effect went beyond the mere negativity of death-reminders, as equally negative-valenced but death-unrelated primes did result in significant vMMRs when combined with enhanced self-perception. We also showed an inverse functional dependency between predictive processing of self and other under death. The weaker the vMMR effect was for the self-death combination, the stronger it was for other-death combination. This is interpreted as an indication that death denial is self-specific; that is involves an alteration of predictive perceptual boundaries between self and other. Finally, a neurophysiological DDI reflecting this relationship was shown to be highly correlated with self-report measures of fear-of-death. We thus interpret these findings as evidence for an early and automatic and death-denying mechanism uniquely attuned to the combination of 'death' and 'self' information.

This death-denial mechanism is compatible with the fMRI literature linking death-related processing to a decrease in self-sentience, mediated by attenuation of insular activity (Han et al., 2010; Klackl et al., 2013; Qin et al., 2018; Shi and Han, 2013). The insula, and in particular its anterior part, is considered to be the main interoceptive hub of the brain (Craig, 2009) that supports a global re-mapping of interoceptive signals underlying conscious access to both subjective feeling and self-related exteroceptive information. As such, it has been suggested to be a comparator mechanism underlying interoceptive inference (Barrett and Simmons, 2015; Critchley and Harrison, 2013; Seth and Friston, 2016), and has been assigned a central role in the generation of pre-reflective minimal forms of selfhood (Craig, 2010; Seth, 2013; Seth et al., 2011; Tsakiris, 2017). The insula and the anterior part of the cingulate cortex

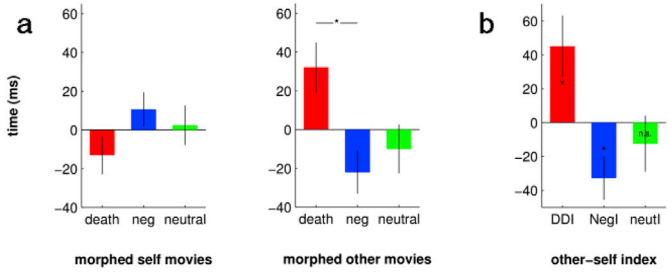

Fig. 7. Identity change RTs for SELF and OTHER morphed clips. Mean corrected response times (y-axis) indicating an identity change in morph clips of (a) self face (left) or an other's face (right), under priming (x-axis) of death, negative and neutral words. (b) Other minus self indices for death (DDI), negative (NegI) and neutral (NeutI) primes. * = $p < .05$
Abbreviations: DDI = death-denial index; NegI = negativity index; NeutI = neutral index.

(ACC) are functionally distinct but often work in tandem (Medford and Critchley, 2010; Menon and Uddin, 2010; Seeley et al., 2007). In particular, they have been described as the limbic system's functional equivalents to the cortex's 'sensory' and 'motor' areas, respectively (Medford and Critchley, 2010; Seth, 2013). Thus, we interpret the present findings which highlighted an attenuated ACC response – a lack of 'motor' command to activate the vMMR – as complementary, and perhaps leading to, a decreased 'sensing' of salience when death and self coincide. Such an experiential avoidance account is coherent with studies showing that death is threatening (Arndt et al., 1998; Guan et al., 2015; Wisman et al., 2015) and salient (Fan and Han, 2018) to the degree that it pertains to the 'self'.

As stated, prediction errors can be resolved by updating priors to best explain incoming sensory information. However, when a prior is deemed too important to relinquish, the brain mounts a second strategy of actively sampling the sensorium in a biased manner compatible with the prediction. Experiment 2 provided evidence of such an active inference mechanism by showing slower latencies of identity change judgments in 'other' morph video clips under death-related priming, enhancing the probabilistic relation between death and the other. In this manner, the biased 'death relates to the other (non-self)' prior can be maintained in the face of reality.

But what are the costs of this psychological fabrication? Immediate defenses against mortality have been shown to tax cognitive resources (Arndt et al., 2007, 1997). Given that death-reminders, even as subtle as a death-related word, are ubiquitous; and given that the process of death-denial affects basic low-level perceptual processes – the degree to which the brain's cognitive capacities might benefit when freed from the imperative of constantly monitoring for and altering the perception of death reminders is an open empirical question. Existential philosophers have long argued that boldly facing the prospects of dying; truly knowing we, rather than everybody else, are going to die, is *the* factor which can summon the mental resources necessary for overcoming a deeply ingrained acculturation and facilitate an existential shift towards a more authentic and meaningful life (Heidegger, 1962; Kierkegaard, 1983).

In sum, we presented novel initial behavioral and neurophysiological evidence revealing a simple but effective prediction-based death-denial mechanism functioning at the level of the brain's self-specific perceptual system. This mechanism can help us understand the gap between the rational certainty that death is inevitable and the experiential tendency to feel the self as an enduring entity. One outstanding question is whether this death-denial mechanism has been positively selected for as a necessary precondition for the evolution of human self-awareness and inter-subjectivity (Qirko, 2017; Varki, 2009; Varki and Brower, 2013), or whether these findings are merely a neural reflection of a death-phobic societal acculturation (Jenkinson, 2015). We acknowledge that the stability of the study's findings and non-findings are limited by the novelty of the paradigms and their sample sizes. They should thus be replicated in further experiments. Looking ahead, the presented framework can be used to scientifically investigate the utility of psychotherapies or contemplative practices targeting death anxiety. We hope that this account of how the brain confronts the notion of its finitude will inspire a robust and theory-driven approach within the emerging field of existential neuroscience.

Conflicts of interest

The authors declare no conflict of interests.

Acknowledgments

This research was conducted in Bar-Ilan University as part of a dissertation towards reception of a Ph.D. in Neuroscience.

References

Aguinis, H., Gottfredson, R.K., Joo, H., 2013. Best-practice recommendations for defining, identifying, and handling outliers. Organ. Res. Methods 16, 270–301. https://doi.org/10.1177/1094428112470848.

Apps, M.A.J., Tsakiris, M., 2014. The free-energy self: a predictive coding account of self-recognition. Neurosci. Biobehav. Rev. 41, 85–97. https://doi.org/10.1016/j.neubiorev.2013.01.029.

Arndt, J., Cook, A., Goldenberg, J.L., Cox, C.R., 2007. Cancer and the threat of death: the cognitive dynamics of death-thought suppression and its impact on behavioral health intentions. J. Personal. Soc. Psychol. 92, 12–29. https://doi.org/10.1037/0022-3514.92.1.12.

Arndt, J., Greenberg, J., Simon, L., Pyszczynski, T., Solomon, S., 1998. Terror management and self-awareness: evidence that mortality salience provokes avoidance of the self-focused state. Personal. Soc. Psychol. Bull. 24, 1216–1227. https://doi.org/10.1177/01461672982411008.

Arndt, J., Greenberg, J., Solomon, S., Pyszczynski, T., Simon, L., 1997. Suppression, accessibility of death-related thoughts, and cultural worldview defense: exploring the psychodynamics of terror management. J. Personal. Soc. Psychol. 73, 5–18. https://doi.org/10.1037/0022-3514.73.1.5.

Baillet, S., 2017. Magnetoencephalography for brain electrophysiology and imaging. Nat. Neurosci. 20, 327–339. https://doi.org/10.1038/nn.4504.

Barrett, L.F., Simmons, W.K., 2015. Interoceptive predictions in the brain. Nat. Rev. Neurosci. 16, 419–429. https://doi.org/10.1038/nrn3950.

Bastiaansen, M.C.M., Knösche, T.R., 2000. Tangential derivative mapping of axial MEG applied to event-related desynchronization research. Clin. Neurophysiol. 111, 1300–1305. https://doi.org/10.1016/S1388-2457(00)00272-8.

Bastos, A.M., Usrey, W.M., Adams, R.A., Mangun, G.R., Fries, P., Friston, K.J., 2012. Canonical microcircuits for predictive coding. Neuron 76, 695–711. https://doi.org/10.1016/j.neuron.2012.10.038.

Bell, A.J., Sejnowski, T.J., 1995. An information-maximization approach to blind separation and blind deconvolution. Neural Comput. 7, 1129–1159. https://doi.org/10.1162/neco.1995.7.6.1129.

Brédart, S., Delchambre, M., Laureys, S., 2006. One's own face is hard to ignore. Q. J. Exp. Psychol. 59, 46–52. https://doi.org/10.1080/17470210500343678.

Brooks, J.L., Zoumpoulaki, A., Bowman, H., 2017. Data-driven region-of-interest selection without inflating Type I error rate. Psychophysiology 54, 100–113. https://doi.org/10.1111/psyp.12682.

Burke, B.L., Martens, A., Faucher, E.H., 2010. Two decades of terror management theory: a meta-analysis of mortality salience research. Personal. Soc. Psychol. Rev. 14, 155–195. https://doi.org/10.1177/1088868309352321.

Christoff, K., Cosmelli, D., Legrand, D., Thompson, E., 2011. Specifying the self for cognitive neuroscience. Trends Cogn. Sci. 15, 104–112. https://doi.org/10.1016/j.tics.2011.01.001.

Clark, A., 2013. Whatever next? Predictive brains, situated agents, and the future of cognitive science. Behav. Brain Sci. 36, 181–204. https://doi.org/10.1017/S0140525X12000477.

Colonnello, V., Chen, F.S., Panksepp, J., Heinrichs, M., 2013. Oxytocin sharpens self-other perceptual boundary. Psychoneuroendocrinology 38, 2996–3002. https://doi.org/10.1016/j.psyneuen.2013.08.010.

Craig, A.D.B., 2010. The sentient self. Brain Struct. Funct. 214, 563–577. https://doi.org/10.1007/s00429-010-0248-y.

Craig, A.D.B., 2009. How do you feel–now? The anterior insula and human awareness. Nat. Rev. Neurosci. 10, 59–70. https://doi.org/10.1038/nrn2555.

Critchley, H.D., Harrison, N.A., 2013. Visceral influences on brain and behavior. Neuron 77, 624–638. https://doi.org/10.1016/j.neuron.2013.02.008.

Dienes, Z., 2014. Using Bayes to get the most out of non-significant results. Front. Psychol. 5. https://doi.org/10.3389/fpsyg.2014.00781.

Eklund, A., Nichols, T.E., Knutsson, H., 2016. Cluster failure: why fMRI inferences for spatial extent have inflated false-positive rates. Proc. Natl. Acad. Sci. 113 (28), 7900–7905. https://doi.org/10.1073/pnas.1602413113.

Fan, X., Han, S., 2018. Neural responses to one's own name under mortality threat. Neuropsychologia 108, 32–41. https://doi.org/10.1016/j.neuropsychologia.2017.11.026.
Florian, V., Kravetz, S., 1983. Fear of personal death: attribution, structure, and relation to religious belief. J. Personal. Soc. Psychol. 44 (3), 600–607. https://doi.org/10.1037/0022-3514.44.3.600.
Garrido, M.I., Kilner, J.M., Stephan, K.E., Friston, K.J., 2009. The mismatch negativity: a review of underlying mechanisms. Clin. Neurophysiol. 120, 453–463. https://doi.org/10.1016/j.clinph.2008.11.029.
Greenberg, J., Kosloff, S., 2008. Terror management theory: implications for understanding prejudice, stereotyping, intergroup conflict, and political attitudes. Soc. Personal. Psychol. Compass 2, 1881–1894. https://doi.org/10.1111/j.1751-9004.2008.00144.x.
Greenberg, J., Pyszczynski, T., Solomon, S., 1986. The causes and consequences of a need for self-esteem: a terror management theory. In: Baumeister, R.R. (Ed.), Public Self and Private Self. Springer-Verlag, New York, pp. 189–212.
Guan, L., Chen, Y., Xu, X., Qiao, L., Wei, J., Han, S., Yang, J., Liu, Y., 2015. Self-esteem buffers the mortality salience effect on the implicit self-face processing. Personal. Individ. Differ. 85, 77–85. https://doi.org/10.1016/J.PAID.2015.04.032.
Hämäläinen, M., Hari, R., Ilmoniemi, R.J., Knuutila, J., Lounasmaa, O.V., 1993. Magnetoencephalography theory, instrumentation, and applications to noninvasive studies of the working human brain. Rev. Mod. Phys. 65, 413–497. https://doi.org/10.1103/RevModPhys.65.413.
Han, S., Qin, J., Ma, Y., 2010. Neurocognitive processes of linguistic cues related to death. Neuropsychologia 48, 3436–3442. https://doi.org/10.1016/j.neuropsychologia.2010.07.026.
Hedge, C., Stothart, G., Todd Jones, J., Rojas Frías, P., Magee, K.L., Brooks, J.C.W., 2015. A frontal attention mechanism in the visual mismatch negativity. Behav. Brain Res. 293, 173–181. https://doi.org/10.1016/j.bbr.2015.07.022.
Heidegger, M., 1962. Being and Time. Blackwell, Oxford, UK.
Heinisch, C., Wiens, S., Gründl, M., Juckel, G., Brüne, M., 2013. Self-face recognition in schizophrenia is related to insight. Eur. Arch. Psychiatry Clin. Neurosci. 263, 655–662. https://doi.org/10.1007/s00406-013-0400-9.
Henry, E. a, Bartholow, B.D., Arndt, J., 2010. Death on the brain: effects of mortality salience on the neural correlates of ingroup and outgroup categorization. Soc. Cogn. Affect. Neurosci. 5, 77–87. https://doi.org/10.1093/scan/nsp041.
Jenkinson, S., 2015. Die Wise: A Manifesto for Sanity and Soul. North Atlantic Books, Berkeley, California.
Jung, T.-P., Makeig, S., Westerfield, M., Townsend, J., Courchesne, E., Sejnowski, T.J., 2000. Removal of eye activity artifacts from visual event-related potentials in normal and clinical subjects. Clin. Neurophysiol. 111, 1745–1758. https://doi.org/10.1016/S1388-2457(00)00386-2.
Keenan, J.P., Freund, S., Hamilton, R.H., Ganis, G., Pascual-Leone, A., 2000. Hand response differences in a self-face identification task. Neuropsychologia 38, 1047–1053. https://doi.org/10.1016/S0028-3932(99)00145-1.
Kierkegaard, S., 1983. Fear and Trembling. Princeton University Press, Princeton, NJ.
Kilner, J.M., 2013. Bias in a common EEG and MEG statistical analysis and how to avoid it. Clin. Neurophysiol. 124 (10), 2062–2063.
Kimura, M., Kondo, H., Ohira, H., Schroger, E., 2012. Unintentional temporal context-based prediction of emotional faces: an electrophysiological study. Cerebr. Cortex 22, 1774–1785. https://doi.org/10.1093/cercor/bhr244.
Kita, Y., Gunji, A., Sakihara, K., Inagaki, M., Kaga, M., Nakagawa, E., Hosokawa, T., 2010. Scanning strategies do not modulate face identification: eye-tracking and near-infrared spectroscopy study. PLoS One 5, e11050. https://doi.org/10.1371/journal.pone.0011050.
Klackl, J., Jonas, E., Kronbichler, M., 2013. Existential Neuroscience: self-esteem moderates neuronal responses to mortality-related stimuli. Soc. Cogn. Affect. Neurosci. 9 (11), 1754–1761. https://doi.org/10.1093/scan/nst167.
Kriegeskorte, N., Simmons, W.K., Bellgowan, P.S., Baker, C.I., 2009. Circular analysis in systems neuroscience: the dangers of double dipping. Nat. Neurosci. 12 (5), 535–540. https://doi.org/10.1038/nn.2303.
Lieder, F., Stephan, K.E., Daunizeau, J., Garrido, M.I., Friston, K.J., 2013. A neurocomputational model of the mismatch negativity. PLoS Comput. Biol. 9, e1003288. https://doi.org/10.1371/journal.pcbi.1003288.
Limanowski, J., Blankenburg, F., 2013. Minimal self-models and the free energy principle. Front. Hum. Neurosci. 7, 547. https://doi.org/10.3389/fnhum.2013.00547.
Litvak, V., Mattout, J., Kiebel, S., Phillips, C., Henson, R., Kilner, J., Barnes, G., Oostenveld, R., Daunizeau, J., Flandin, G., Penny, W., Friston, K., 2011. EEG and MEG data analysis in SPM8. Comput. Intell. Neurosci. 2011, 852961. https://doi.org/10.1155/2011/852961.
Luck, S.J., Gaspelin, N., 2017. How to get statistically significant effects in any ERP experiment (and why you shouldn't). Psychophysiology 54, 146–157. https://doi.org/10.1111/psyp.12639.
Maris, E., Oostenveld, R., 2007a. Nonparametric statistical testing of EEG-and MEG-data. J. Neurosci. Methods 164, 177–190.
Maris, E., Oostenveld, R., 2007b. Nonparametric statistical testing of EEG- and MEG-data. J. Neurosci. Methods 164, 177–190. https://doi.org/10.1016/j.jneumeth.2007.03.024.
Medford, N., Critchley, H.D., 2010. Conjoint activity of anterior insular and anterior cingulate cortex: awareness and response. Brain Struct. Funct. 214, 535–549. https://doi.org/10.1007/s00429-010-0265-x.
Menon, V., Uddin, L.Q., 2010. Saliency, switching, attention and control: a network model of insula function. Brain Struct. Funct. 214, 655–667. https://doi.org/10.1007/s00429-010-0262-0.
Miyakoshi, M., Kanayama, N., Iidaka, T., Ohira, H., 2010. EEG evidence of face-specific visual self-representation. Neuroimage 50, 1666–1675. https://doi.org/10.1016/j.neuroimage.2010.01.030.
Oostenveld, R., Fries, P., Maris, E., Schoffelen, J.-M., 2011. FieldTrip: open source software for advanced analysis of MEG, EEG, and invasive electrophysiological data. Comput. Intell. Neurosci. 1–9, 2011. https://doi.org/10.1155/2011/156869.
Pannese, A., Hirsch, J., 2010. Self-specific priming effect. Conscious. Cognit. 19, 962–968. https://doi.org/10.1016/j.concog.2010.06.010.
Platek, S.M., Loughead, J.W., Gur, R.C., Busch, S., Ruparel, K., Phend, N., Panyavin, I.S., Langleben, D.D., 2006. Neural substrates for functionally discriminating self-face from personally familiar faces. Hum. Brain Mapp. 27, 91–98. https://doi.org/10.1002/hbm.20168.
Platek, S.M., Wathne, K., Tierney, N.G., Thomson, J.W., 2008. Neural correlates of self-face recognition: an effect-location meta-analysis. Brain Res. 1232, 173–184. https://doi.org/10.1016/j.brainres.2008.07.010.
Poldrack, R.A., 2006. Can cognitive processes be inferred from neuroimaging data? Trends Cogn. Sci. 10, 59–63. https://doi.org/10.1016/j.tics.2005.12.004.
Pyszczynski, T., Greenberg, J., Solomon, S., Arndt, J., Schimel, J., 2004. Why do people need self-esteem? A theoretical and empirical review. Psychol. Bull. 130, 435–468. https://doi.org/10.1037/0033-2909.130.3.435.
Pyszczynski, T., Solomon, S., Greenberg, J., 2015. Thirty years of terror management theory. In: Advances in Experimental Social Psychology, pp. 1–70. https://doi.org/10.1016/bs.aesp.2015.03.001.
Qin, J., Shi, Z., Ma, Y., Han, S., 2018. Gender and neural substrates subserving implicit processing of death-related linguistic cues. Cogn. Process. 1. https://doi.org/10.1007/s10339-017-0847-0.
Qirko, H.N., 2017. An evolutionary argument for unconscious personal death unawareness. Mortality 22, 255–269. https://doi.org/10.1080/13576275.2016.1176018.
Rao, R.P.N., Ballard, D.H., 1999. Predictive coding in the visual cortex: a functional interpretation of some extra-classical receptive-field effects. Nat. Neurosci. 2, 79–87. https://doi.org/10.1038/4580.
Ratcliff, R., 1993. Methods for dealing with reaction time outliers. Psychol. Bull. 114, 510–532. https://doi.org/10.1037/0033-2909.114.3.510.
Sedikides, C., Gregg, A.P., 2008. Self-enhancement: food for thought. Perspect. Psychol. Sci. 3, 102–116. https://doi.org/10.1111/j.1745-6916.2008.00068.x.
Seeley, W.W., Menon, V., Schatzberg, A.F., Keller, J., Glover, G.H., Kenna, H., Reiss, A.L., Greicius, M.D., 2007. Dissociable intrinsic connectivity networks for salience processing and executive control. J. Neurosci. 27, 2349–2356. https://doi.org/10.1523/JNEUROSCI.5587-06.2007.
Sel, A., Harding, R., Tsakiris, M., 2016. Electrophysiological correlates of self-specific prediction errors in the human brain. Neuroimage 125, 13–24. https://doi.org/10.1016/j.neuroimage.2015.09.064.
Seth, A.K., 2013. Interoceptive inference, emotion, and the embodied self. Trends Cogn. Sci. 17, 565–573. https://doi.org/10.1016/j.tics.2013.09.007.
Seth, A.K., Friston, K.J., 2016. Active interoceptive inference and the emotional brain. Philos. Trans. R. Soc. Biol. Sci. 371, 20160007. https://doi.org/10.1098/rstb.2016.0007.
Seth, A.K., Suzuki, K., Critchley, H.D., 2011. An interoceptive predictive coding model of conscious presence. Front. Psychol. 2, 395. https://doi.org/10.3389/fpsyg.2011.00395.
Shay, E., 2016. Initial Processing of Death-Related Stimuli. Bar-Ilan University.
Shi, Z., Han, S., 2013. Transient and sustained neural responses to death-related linguistic cues. Soc. Cogn. Affect. Neurosci. 8, 573–578. https://doi.org/10.1093/scan/nss034.
Stefanics, G., Csukly, G., Komlósi, S., Czobor, P., Czigler, I., 2012. Processing of unattended facial emotions: a visual mismatch negativity study. Neuroimage 59, 3042–3049. https://doi.org/10.1016/j.neuroimage.2011.10.041.
Stefanics, G., Jan Czigler, I., 2014a. Visual mismatch negativity: a predictive coding view. Front. Hum. Neurosci. 8. https://doi.org/10.3389/fnhum.2014.00666.
Stefanics, G., Kremláček, J., Czigler, I., 2014b. Visual mismatch negativity: a predictive coding view. Front. Hum. Neurosci. 8. https://doi.org/10.3389/fnhum.2014.00666.
Tajadura-Jiménez, A., Tsakiris, M., 2014. Balancing the "inner" and the "outer" self: interoceptive sensitivity modulates self–other boundaries. J. Exp. Psychol. Gen. 143, 736–744. https://doi.org/10.1037/a0033171.
Tal, I., Abeles, M., 2013. Cleaning MEG artifacts using external cues. J. Neurosci. Methods 217, 31–38. https://doi.org/10.1016/j.jneumeth.2013.04.002.
Tsakiris, M., 2017. The multisensory basis of the self: from body to identity to others. Q. J. Exp. Psychol. 70, 597–609. https://doi.org/10.1080/17470218.2016.1181768.
Van Veen, B.D., van Drongelen, W., Yuchtman, M., Suzuki, A., 1997. Localization of brain electrical activity via linearly constrained minimum variance spatial filtering. IEEE Trans. Biomed. Eng. 44, 867–880. https://doi.org/10.1109/10.623056.
Varki, A., 2009. Human uniqueness and the denial of death. Nature 460, 684. https://doi.org/10.1038/460684c.
Varki, A., Brower, D., 2013. Denial: Self Deception, False Beliefs, and the Origins of the Human Mind. Twelve, New York.
Vogel, B.O., Shen, C., Neuhaus, A.H., 2015. Emotional context facilitates cortical prediction error responses. Hum. Brain Mapp. 36, 3641–3652. https://doi.org/10.1002/hbm.22868.
Willenbockel, V., Sadr, J., Fiset, D., Horne, G.O., Gosselin, F., Tanaka, J.W., 2010. Controlling low-level image properties: the SHINE toolbox. Behav. Res. Methods 42, 671–684. https://doi.org/10.3758/BRM.42.3.671.
Winkler, I., Czigler, I., 2012. Evidence from auditory and visual event-related potential (ERP) studies of deviance detection (MMN and vMMN) linking predictive coding

theories and perceptual object representations. Int. J. Psychophysiol. 83, 132–143. https://doi.org/10.1016/j.ijpsycho.2011.10.001.

Wisman, A., Heflick, N., Goldenberg, J.L., 2015. The great escape: the role of self-esteem and self-related cognition in terror management. J. Exp. Soc. Psychol. 60, 121–132. https://doi.org/10.1016/j.jesp.2015.05.006.

Xu, Q., Ruohonen, E.M., Ye, C., Li, X., Kreegipuu, K., Stefanics, G., Luo, W., Astikainen, P., 2018. Automatic processing of changes in facial emotions in dysphoria: a magnetoencephalography study. Front. Hum. Neurosci. 12, 186. https://doi.org/10.3389/fnhum.2018.00186.